Is there still any T_c mystery in lattice QCD?
Results with physical masses in the continuum limit III

Szabolcs Borsányi[a]*, **Zoltán Fodor**[a,b,c], **Christian Hoelbling**[a], **Sándor D. Katz**[c], **Stefan Krieg**[a,d], **Claudia Ratti**[a] and **Kálmán K. Szabó**[a]

[a]*Department of Physics, University of Wuppertal, Gaußstr. 20, D-42119, Germany*
[b]*John von Neumann Institute for Computing, Jülich, D-52425, Germany*
[c]*Institute for Theoretical Physics, Eötvös University, Pázmány 1, H-1117 Budapest, Hungary*
[d]*Center for Theoretical Physics, MIT, Cambridge, MA 02139-4307, USA*

ABSTRACT: The present paper concludes our investigations on the QCD cross-over transition temperatures with 2+1 staggered flavours and one-link stout improvement. We extend our previous two studies [Phys. Lett. B643 (2006) 46, JHEP 0906:088 (2009)] by choosing even finer lattices (N_t=16) and we work again with physical quark masses. The new results on this broad cross-over are in complete agreement with our earlier ones. We compare our findings with the published results of the hotQCD collaboration. All these results are confronted with the predictions of the Hadron Resonance Gas model and Chiral Perturbation Theory for temperatures below the transition region. Our results can be reproduced by using the physical spectrum in these analytic calculations. The findings of the hotQCD collaboration can be recovered by using a distorted spectrum which takes into account lattice discretization artifacts and heavier than physical quark masses. This analysis provides a simple explanation for the observed discrepancy in the transition temperatures between our and the hotQCD collaborations.

KEYWORDS: QCD transition, Lattice QCD.

*borsanyi@uni-wuppertal.de

Contents

1. Introduction

In recent years, increasing attention has been devoted to study the properties of the QCD phase diagram and thermodynamics. On the one hand, the heavy ion collision experiments at CERN SPS, RHIC at Brookhaven National Laboratory and ALICE at the Large Hadron Collider (LHC) provide the unique possibility of quantifying the properties of the deconfined phase of QCD. On the other hand, lattice calculations on QCD thermodynamics are reaching unprecedented levels of accuracy, with simulations at the physical quark masses and several values of the lattice cutoff: this allows to keep lattice artifacts under control. The information that can be obtained from these complementary approaches will shed light on the features of QCD matter under extreme conditions, one of the major challenges of the physics of strong interaction.

One of the most interesting quantities that can be extracted from lattice simulations is the transition temperature T_c at which hadronic matter is supposed to undergo a transition to a deconfined, quark-gluon phase. This quantity has been vastly debated over the last few years, due to the disagreement on its numerical value observed by different lattice collaborations, which in some cases is as high as 20% of the absolute value. Indeed, the analysis of the hotQCD collaboration (performed with two different improved staggered

fermion actions, asqtad and p4, and with physical strange quark mass and somewhat larger than physical u and d quark masses, $m_s/m_{u,d} = 10$), indicates that the transition region lies in the range $T = (185 - 195)$ MeV. Different observables lead to the same value of T_c [1, 2, 3, 4, 5]. Recent simulations using the p4 action with the quark mass ratio $m_s/m_u = 20$ yielded about 5 MeV shift (towards the smaller values) in the temperature dependence of the studied observables [6]. On the other hand, the results obtained by our collaboration using the staggered stout action (with physical light and strange quark masses, thus $m_s/m_{u,d} \simeq 28$) are quite different: the value of the transition temperature lies in the range 150-170 MeV, and it changes with the observable used to define it [7, 8]. This is not surprising, since the transition is a cross-over [9]: in this case it is possible to speak about a transition region, in which different observables may have their characteristic points at different temperature values, and the temperature dependences of the various observables play a more important role than any single T_c value. Unfortunately, the 25-30 MeV discrepancy was observed between the two collaborations for the T dependences of the various observables, too.

A lot of effort has been invested, in order to find the origin of the discrepancy between the results of the two collaborations.[1] In Refs. [7, 8], we emphasized the role of the proper continuum limit with physical quark masses, showing how the lack of them can distort the result. In [12] we pointed out that the continuum limit can be approached only if one reduces the unphysical pion splitting (the main motivation of our choice of action). An interesting application of these observations was studied in [13]. These authors have performed an analysis of trace anomaly, strangeness and baryon number fluctuations within the Hadron Resonance Gas model (HRG). They show that, to reproduce the lattice results for the asqtad and p4 actions of the hotQCD collaboration, it is necessary to distort the resonance spectrum away from the physical one in order to take into account the larger quark masses used in these lattice calculations, as well as finite lattice spacing effects. As we will see, no such distortion is needed to describe our data, and the discrepancy between the two collaborations has its roots in the above mentioned lattice artifacts. In the present paper we perform a similar analysis for those quantities that can be calculated in the HRG model and Chiral Perturbation Theory (χPT), namely the chiral condensate, the strange quark susceptibility and the equation of state. From the lattice point of view, we present our most recent results for several physical quantities: our previous calculations [7, 8] have been extended to an even smaller lattice spacing (down to $a \lesssim 0.075$ fm in the transition region), corresponding to $N_t = 16$. We use physical light and strange quark masses: we fix them by reproducing f_K/m_π and f_K/m_K and by this procedure [8] we get $m_s/m_{u,d} = 28.15$. The HRG model results are obtained both for the physical resonance masses, as listed in the Particle Data Book, and for the distorted spectrum which corresponds to the quark masses and finite lattice spacings of [5]. Our analysis indicates that the discretization effects on hadron masses (and in particular on the nondegenerate, taste-split light pseudoscalar meson masses which emerge as a consequence of the staggered formalism) affect more severely the asqtad and p4 actions than the stout one, in the temperature regime below and around

---

[1]Note, that quite recently preliminary results were presented [10, 11] and the results of the hotQCD collaboration moved closer to our results. (We include some of these data in our comparisons.)

T_c. Indeed, the lattice results obtained with the stout action show a very good agreement with the HRG model results with physical quark masses, while the lattice results obtained with the asqtad and p4 actions can be reproduced within the HRG model only with the distorted spectrum. The discrepancy in the transition temperature values obtained by the two collaborations can be easily explained by this result.

The paper is organized as follows. In Section 2 we give a brief review of the qualitative features of the QCD transition (those who are interested more in the qualitative features than in the technicalities might read this section and then jump directly to subsection 5.2). In Section 3 we give the details of our numerical simulations. In Section 4 we present the results of our simulations for different observables. In Section 5 we present some aspects of the Hadron Resonance Gas model and the comparison between lattice and HRG model results. We write our Conclusions in Section 6. In Appendix A we provide some details of the chiral condensate calculation in the HRG model + χPT. Appendix B presents the temperature dependence of our continuum extrapolated lattice results.

2. The QCD transition

In this section we summarize the qualitative features of the $T > 0$ QCD transition. One of the most important pieces of information we have is our knowledge about the nature of the transition. Though many take it for granted, it is a higly non-trivial result, that the transition is an analytic one and usually called a cross-over [9]. In order to show this by means of lattice QCD, physical quark masses were taken, and a finite size scaling analysis was carried out for the continuum extrapolated chiral susceptibilities. This analytic behaviour has important consequences for any T_c determination in QCD.

In order to illustrate the most important differences between a real phase transition and an analytic cross-over, we recall the water-vapor phase diagram on the temperature versus pressure plane (c.f. [7] and Figure 1 of the present paper). We study the transition by fixing the pressure to a given value and then varying the temperature. For smaller pressures (p$\lesssim$22 MPa) there is a first order phase transition. The density jumps, the heat capacity is infinite, and these singular features appear simultenously, thus exactly at the same critical temperature. At pressure $p \approx$22.064 MPa and temperature $T \approx$647.096 K, there is a critical point with a second order phase transition. This phase transition is also characterized by a singular behaviour. [2]

At even larger pressures (p$\gtrsim$22.064 MPa) the water-vapor transition is an analytic one (the behaviours of various observables are analytic, even in the infinite volume limit). As a consequence, in this pressure region there is no jump in the density when we change the temperature, only a rapid but continuous change. The inflection point of this density-temperature function (the point with the largest, though finite, derivative) can be used to define the pseudocritical temperature (another usual name for it is "transition temperature") related to the density. Similarly, the heat capacity is always finite, but it has a

---

[2]Note, that a real singularity, a phase transition, takes place only in infinite size systems. In our example we have a macroscopic amount of water with $O(10^{23})$ molecules. From the practical point of view, this is an infinitely large system.
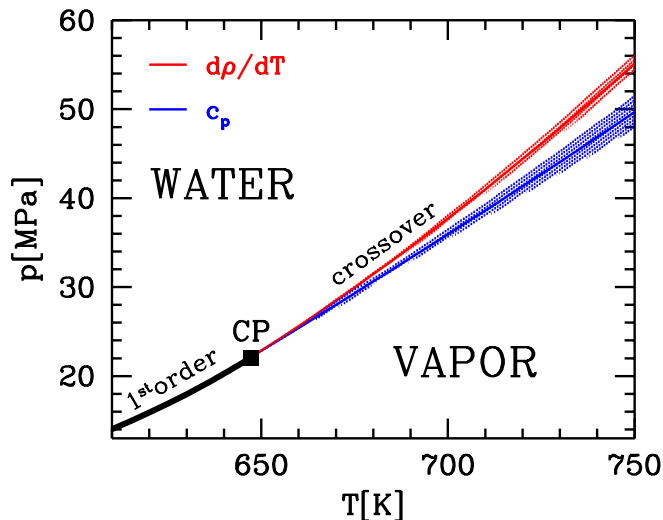
Figure 1: The phase diagram of water around its critical point (CP). For pressures below the critical value (p_c) the transition is first order, for $p > p_c$ values there is a rapid cross-over. In the cross-over region the critical temperatures defined from different quantities are not necessarily equal. This can be seen for the temperature derivative of the density $(d\rho/dT)$ and the specific heat (c_p). The bands show the non-negligible experimental uncertainties (see [14]).

pronounced peak as we increase the temperature. The position of this peak can be used to define the pseudocritical temperature related to the heat capacity. Despite the fact that there is no singularity, the inflection point and peak position are well defined. The corresponding pseudocritical or transition temperature is usually denoted as T_c.

The most important message here is that the various transition temperatures (e.g. those related to the density or heat capacity) behave differently depending on whether we are in the singular (real phase transition) or non-singular (analytic cross-over) region. As it is indicated on the figure, for a real phase transition these critical temperatures coincide, whereas in the non-singular region (for pressures above 22.064 MPa) the pseudocritical temperatures can differ considerably. The fast change (though no jump) in the density is at a lower temperature than the peak in the heat capacity. The transition is a broad cross-over. The pseudocritical temperatures, related to various observables, are separated, but both of them are in the broad transition temperature region. This separation does not mean that we have two transitions (one for the density and one for the heat capacity), it merely reflects the broadness of the transition.

It is easy to see that different observables can give different pseudocritical temperatures. Let us study an observable X, which characterizes the transition as a function of the temperature $X(T)$. For a real phase transition its singular behaviour appears at the same temperature even if we multiplied it by T (an infinitely high peak keeps its position). For an analytic cross-over, we have a peak with a finite height and a finite width. Multiplying it by T shifts the peak position to larger temperature values. The value of T_c is shifted.

The pseudocritical temperature is well defined for any definition, but it is not unique. Furthermore, for a broad transition the whole neighbourhood of the peak behaves similarly as the peak, the determination of the peak's or inflexion point's position is difficult (this is the experimental reason for the uncertainties on Figure 1 and this technical difficulty is present for the even broader QCD transition). Though a T_c related to some observable is informative, a more complete description is given by the whole temperature dependence of $X(T)$.

The determination of such curves is the main goal of any study on the QCD transition (c.f. our earlier studies [7, 8]). Since the QCD transition (at vanishing chemical potential) is an analytic cross-over, one wants to obtain these smooth curves for several observables. Though the characteristic points of such curves contain obviously less information than the curves themselves, we give them, too.

Before we list the observables we study in detail, it is worth mentioning that the cross-over nature of the QCD transition is related to the specific values of the quark masses we have in nature. For two- or three-flavour QCD with vanishing quark masses or with infinitely massive quarks, one is supposed to have real phase transitions. There are order parameters (in the former case the chiral susceptibility/condensate signaling the chiral phase transition; in the latter case the Polyakov line signaling the deconfinement phase transition) which show a non-analytic behaviour as we change the temperature. As we pointed out earlier, the highly non-trivial result about the analytic nature of the QCD transition with physical quark masses implies, that no observable can be treated as an order parameter. All of the observables show analytic temperature dependences. There is neither a chiral nor a deconfinement phase transition. Note however, that similarly to the density or to the heat capacity in the water-vapor cross-over transition, the observables chiral susceptibility/condensate and the Polyakov line can develop a pronounced peak or show a rapid change. The peak positions or the inflection points for such a cross-over are usually expected to be at different temperatures. Again, we do not say [7, 8] that there are two phase transitions and one of them is at a lower temperature than the other. The separation of the pseudocritical temperatures is merely a sign of the broad analytic transition [9].

Since the chiral susceptibility/condensate and the Polyakov loop are not order parameters, they are just used to signal the cross-over. In principle any other quantity showing rapid changes or developing a peak in the transition region can be studied. The temperature dependences of these observables can be compared with the predictions of other lattice results or model calculations. In this paper we extend our analysis to new observables and to even finer lattices. We study the above chiral/deconfinement observables and in addition we look at the strange quark number susceptibility and at the energy density or trace anomaly [15].

The reason for calculating the temperature dependence of these many observables is obvious. The more observables we study, the broader picture we have on the QCD transition. To be more specific, the chiral susceptibility/condensate and the Polyakov loop are remnants of the real phase transition order parameters (for other mass regions of the phase plane). In addition to our old observables we use a new definition for the chiral

condensate, which has adventageous renormalization features and gives a result with little noise (due to construction, the chiral susceptibility is somewhat noisy). The strange quark number susceptibility is a particularly attractive quantity from the theoretical point of view. It is related to a conserved current, thus no renormalization ambiguities appear, which makes direct comparisons particularly easy. For a first order phase transition, the energy density has a jump. In the cross-over region the remnant of this jump is an inflection point. Furthermore, the transition temperature related to the equation of state has a direct link to experiments, its importance is obvious.

The various obsevables (listed in the previous paragraph) lead to different transition temperatures, they are typically between 150 and 170 MeV, thus well within the broadness of the transition. Let us emphasize again, the difference between the pseudocritical T_c values does not mean that one of the phase transitions happens at a lower temperature than the other, quite the contrary: no phase transition happens at all. Our new results confirm our earlier findings and their interpretation by all means: the transition temperatures scatter within the broad temperature interval, characteristic of the cross-over.

3. Details of the lattice simulations

3.1 Action, algorithm and scale setting

The lattice action is the same as we used in [7, 8], namely a tree-level Symanzik improved gauge, and a stout-improved staggered fermionic action (see Ref. [16] for details). The stout-smearing [17] reduces the taste violation (see Section 3.2): this kind of smearing has the smallest taste violation among the ones used so far in the literature for large scale thermodynamical simulations[3]. The supression of this artefact is important in the transition region (see the important consequences within the hadron resonance model framework) and that was the main motivation for this choice. For details about the algorithm we refer the reader to [8].

In analogy with what we did in [7, 8], we set the scale at the physical point by simulating at $T = 0$ with physical quark masses [8] and reproducing the kaon and pion masses and the kaon decay constant. This gives an uncertainty of about 2% in the scale setting, which propagates in the uncertainty in the determination of the temperature values listed.

3.2 Taste violation

Most of the large scale QCD thermodynamics studies apply the staggered formalism for the quark fields. Working at non-vanishing lattice spacing within this framework, there is only one single pseudo-Goldstone boson (instead of the experimentally observed three pions). By pseudo-Goldstone we mean a particle whose mass approaches zero if we tune the mass of the quark to zero (note, that in lattice studies usually we do not approach this zero mass –chiral– limit, but we tune the quark masses to their physical values). In addition to this

---

[3]Only recently, first exploratory studies of the hotQCD Collaboration with the HISQ action [10, 11] start to appear: in this case, the projected smeared links improve the taste symmetry in a similar way as in our stout action.

single pseudo-Goldstone boson, there is a whole tower of non-Goldstones. They are usually much heavier, which is a non-physical lattice artifact. The typical mass gap can be as large as several hundred MeV, which vanishes as the lattice spacing tends to zero and one recovers the experimentally observed spectrum (since the original staggered formulation provides four flavours –or how they are called in lattice QCD: tastes– the proper number of degrees of freedom is reached by taking the root of the fermion determinant). On the more formal level, this implies that every pseudoscalar meson (for example pions and kaons) is split into 16 non-degenerate mesons, which can be grouped into the eight multiplets [18] listed in Table 1. Their masses can be written as:

$$m_i^2 = m_0^2 + (\delta m_i)^2. \tag{3.1}$$

The splittings $(\delta m_i)^2$ are proportional to $(\alpha_s a^2)$ for small lattice spacings. Only one out of the 16 pseudoscalar mesons is a true Goldstone boson in the chiral limit. The splitting (the taste symmetry violation) has to vanish in the continuum limit. Once it shows an $\alpha_s a^2$ dependence (in practice a quadratic dependence with a subdominant logarithmic correction) we are in the scaling region. This is an important check for the validity of the staggered framework at a given lattice spacing (for large lattice spacings its behaviour can mimic an incorrect continuum limit). In Ref. [8] we showed a continuum extrapolation of the quadratic mass difference $(\delta m_i)^2$, concluding that the splitting obtained with

index	Γ^F	multiplicity n_i
0	γ_5	1
1	$\gamma_0\gamma_5$	1
2	$\gamma_i\gamma_5$	3
3	$\gamma_i\gamma_j$	3
4	$\gamma_i\gamma_0$	3
5	γ_i	3
6	γ_0	1
7	1	1

Table 1: Left column: index shown in Fig. 2. Central column: taste matrices Γ^F. Right column: multiplicity of the different pseudoscalar mesons.

the stout action is consistent with zero in the continuum limit. We also showed that lattice spacings which are larger than $a \sim 0.15$ fm are not in the expected a^2-scaling regime. In Fig. 2 we show the leading order a^2-behavior of the masses of the pion multiplets calculated with the asqtad (left panel) and stout (right panel) actions. It is evident that the continuum expectation is reached faster in the stout action than in the asqtad one. In addition, in the present paper we push our results to $N_t = 16$, which corresponds to even smaller lattice spacings and mass splittings than those used in [8]. From Fig. 2, we can obtain the lattice spacing-dependent spectrum that we will include in the HRG model, in order to take into account lattice discretization effects.

4. Lattice results

In this Section we present our lattice results for the strange quark number susceptibility, Polyakov loop and two different definitions of the chiral condensate. After performing a continuum extrapolation, we extract the values of the transition temperature associated to these observables. As we alreay emphasized the temperature dependence of an observable contains much more information than the location of a peak or inflection point (which are usually hard to determine precisely for such a broad transition). We perform a HRG
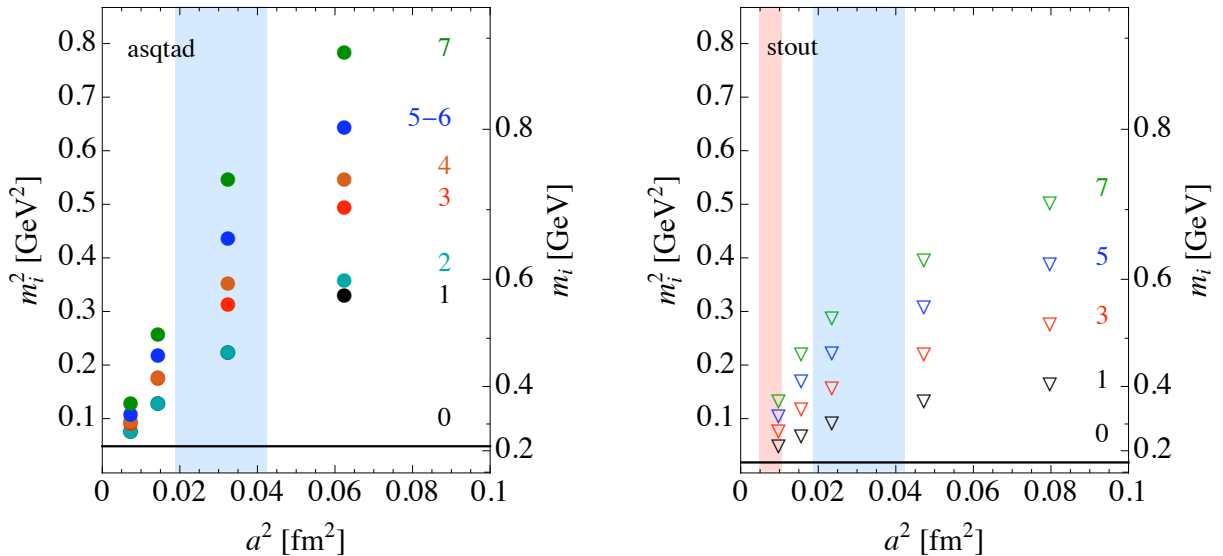
Figure 2: Masses of the pion multiplet squared, as functions of the lattice spacing squared. Left panel: asqtad action [19]. Right panel: stout action. The numbers next to the data correspond to the taste matrices, as listed in Table 1. In both panels, the blue band indicates the relevant range of lattice spacings for a thermodynamics study at $N_t = 8$ between $T = 120$ and 180 MeV. The red band in the right panel corresponds to the same temperature range and $N_t = 16$. In both figures, the horizontal line labelled as "0" is the pseudo-Goldstone boson, which has a mass of 220 MeV for the asqtad results, and 135 MeV for the stout ones (As we mentioned the splitting is formally proportional to $\alpha_s a^2$. At present accuracies and for illustrative purposes the subdominant logarithmic dependence can be omitted).

analysis and compare our results with those of the hotQCD Collaboration in the next Section.

Quark number susceptibilities are defined in the following way:

$$\chi_2^q = \frac{T}{V} \frac{\partial^2 \ln Z}{\partial(\mu_q)^2}\bigg|_{\mu_i=0}, \qquad q = u, d, s. \tag{4.1}$$

These quantities rapidly increase during the transition, therefore they can be used to identify this region. However, while light quark susceptibilities are dominated by pions at small temperatures, kaons are the lightest degrees of freedom for strange quark susceptibilities in the hadronic phase. Therefore, these two quantities are known to behave very differently as functions of the temperature, with the strange quark number susceptibility rising more slowly in the transition region. Due to the presence of disconnected diagrams, the light quark number susceptibility is known to be very noisy and was not calculated. Nevertheless, we will discuss its temperature dependence within the hadron resonance gas model in the next Section.

In the left panel of Fig. 3 we show our results for the strange quark number susceptibility for $N_t = 10, 12, 16$. The gray band is the continuum extrapolation that we have performed using our data: the numerical values are listed in the Table of Appendix B (the

width of this band and those for other observables indicate the statistical and systematic uncertainties of the continuum extrapolation).

The Polyakov loop is the order parameter related to the deconfinement phase transition of QCD in the pure gauge sector. In this case, the Z_3 symmetry is exact at small temperatures, where the Polyakov loop expectation value is zero. In the deconfined phase, this symmetry is spontaneously broken by the expectation value of the Polyakov loop, which jumps to a finite value. When quarks are included in the system, the Z_3 symmetry is explicitly broken by their presence. In this case, the Polyakov loop is no longer a real order parameter. Nevertheless, it is still considered as an indicator for the transition, since it exhibits a rise in the transition region. This is evident from the right panel of Fig. 3, where we plot the renormalized Polyakov loop as a function of the temperature. The need to renormalize it comes from the fact that there are self-energy contributions to the static quark free energy that need to be eliminated. To that end, we use our renormalization procedure of [7]. In order to compare our results with those obtained by the hotQCD collaboration [5] (which will be done in the next Section), the renormalization constant is obtained slightly differently from the condition $V(1.5r_0) = V_{\text{string}}(1.5r_0)$ where V is the zero temperature quark-antiquark potential and $V_{\text{string}}(r) = -\pi/12r + \sigma r$. In addition, we included the factor $\frac{1}{3}$ in the trace definition.

The right panel of Figure 3 shows the different N_t data sets together with the continuum extrapolated result, for which we give numerical data in the Table of Appendix B. As it is expected from a broad cross-over the rise of the Polyakov loop is pretty slow as we increase the temperature (c.f. [5, 7, 8]).
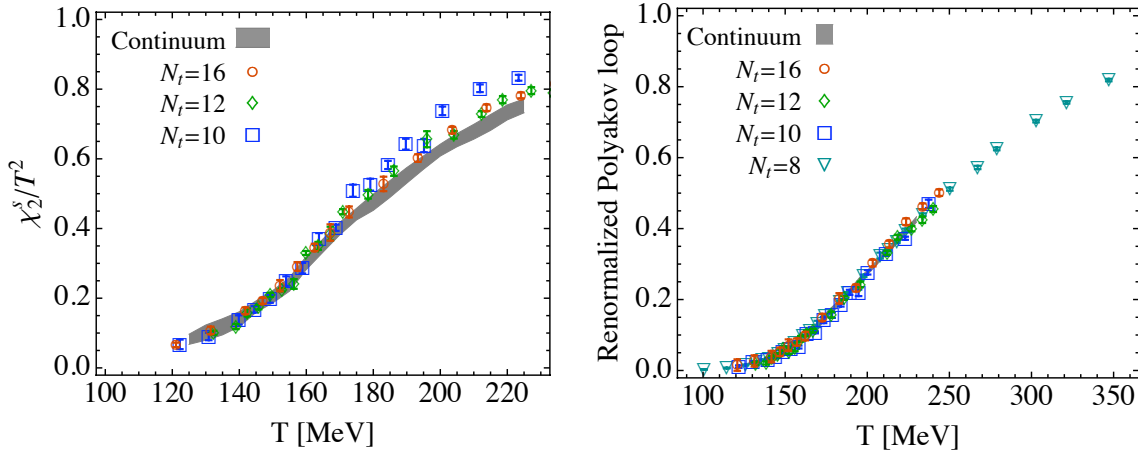

Figure 3: Left: strange quark number susceptibility as a function of the temperature. Right: renormalized Polyakov loop as a function of the temperature. In both figures, the different symbols correspond to different N_t. The gray band is the continuum extrapolated result.

The chiral condensate is defined in the following way:

$$\langle \bar{\psi}\psi \rangle_q = \frac{T}{V} \frac{\partial \ln Z}{\partial m_q}, \qquad q = u, d, s. \tag{4.2}$$

In the case of a real chiral phase transition, the chiral condensate is the corresponding order parameter. However, with physical quark masses there is no real phase transition,
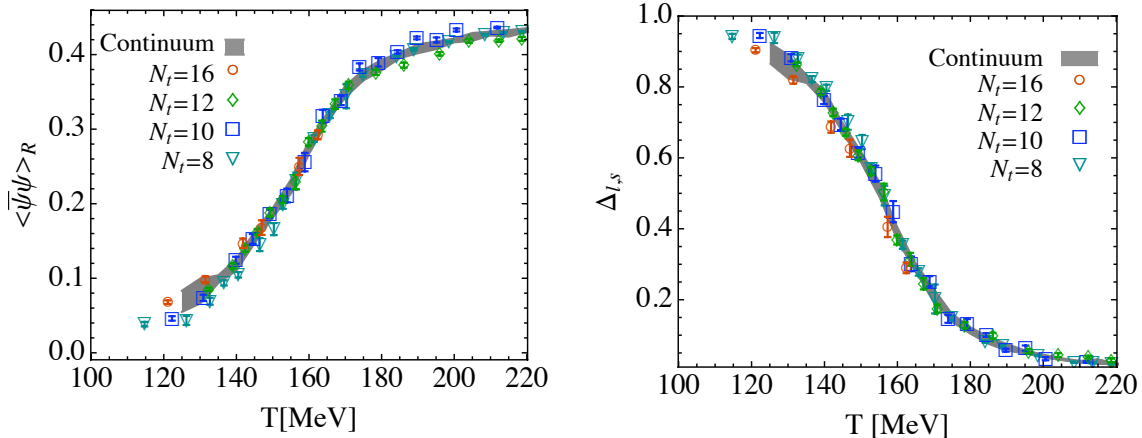
Figure 4: Left: renormalized chiral condensate $\langle\bar{\psi}\psi\rangle_R$ defined in Eq. (4.3). Right: subtracted chiral condensate $\Delta_{l,s}$ defined in Eq. (4.4). In both figures, the different symbols correspond to different N_t. The gray band is our continuum estimate.

just a cross-over. The chiral condensate can still be taken as an indicator for the remnant of the chiral transition, since it rapidly changes in the transition region.

In the present paper, the following definition of the renormalized chiral condensate is used:

$$\langle\bar{\psi}\psi\rangle_R = -\left[\langle\bar{\psi}\psi\rangle_{l,T} - \langle\bar{\psi}\psi\rangle_{l,0}\right]\frac{m_l}{X^4} \qquad l = u, d. \tag{4.3}$$

In the above equation, X can be any quantity which has a dimension of mass. Since we are working with non-vanishing quark masses, m_π is a reasonable choice. This quantity is properly renormalized and the continuum limit can be safely taken [9]. The individual results and the continuum extrapolation are shown in Figure 4.

In order to compare our results to those of the hotQCD collaboration, we also calculate the quantity $\Delta_{l,s}$, which is defined as

$$\Delta_{l,s} = \frac{\langle\bar{\psi}\psi\rangle_{l,T} - \frac{m_l}{m_s}\langle\bar{\psi}\psi\rangle_{s,T}}{\langle\bar{\psi}\psi\rangle_{l,0} - \frac{m_l}{m_s}\langle\bar{\psi}\psi\rangle_{s,0}} \qquad l = u, d. \tag{4.4}$$

Since the results at different lattice spacings are essentially on top of each other, we connect them to lead the eye and use this band in later comparisons (c.f. Fig. 4).

In this section we presented our primary results, the temperature dependence of various observables the same way as we did in our previous works [7, 8]. We found a complete agreement. For the readers' convenience we tabulate the results in the Table of Appendix B. These curves contain the complete information on the observables. Nevertheless, it is usual to determine some characteristic points of these curves (inflection points or peaks). Since the transition is a broad cross-over, these T_c values scatter within the transition range (c.f. Table 2, where we also review the results of our previous analyses for comparison).

For completeness we discuss the trace anomaly too (see next section) and give the transition temperature obtained from it and from the energy density in Table 2 (the details of the equation of state at $N_t = 6, 8, 10$ and 12 will be given in a subsequent publication

	$\chi_{\bar{\psi}\psi}/T^4$	$\Delta_{l,s}$	$\langle\bar{\psi}\psi\rangle_R$	χ_2^s/T^2	ϵ/T^4	$(\epsilon-3p)/T^4$
this work	147(2)(3)	157(3)(3)	155(3)(3)	165(5)(3)	157(4)(3)	154(4)(3)
our work '09	146(2)(3)	155(2)(3)	-	169(3)(3)	-	-
our work '06	151(3)(3)	-	-	175(2)(4)	-	-

Table 2: The pseudocritical temperatures in MeV (defined as the inflection point or peak position of the T dependent observables listed in Section 2) for physical quark masses in the continuum limit. The T_c values from the equation of state (energy density and trace anomaly) are not continuum extrapolated, they are obtained on $N_t = 8$ lattices. We expect a shift within the error bars in the continuum limit. A comparison between our present and earlier results [7] and [8] is given. A change in the experimental f_K value in 2008 resulted in a ≈6 MeV reduction of our T_c predictions (lattice results are unaltered). To compare our results with those of the hotQCD Collaboration a new definition for the Polyakov loop was applied, thus a direct comparison with Refs. [7] and [8] is not possible. As we emphasized, the various T_c values do not indicate separate phase transitions but the broadness of the cross-over. Thus, it is more informative to look at the complete T dependence of the observables (see the figures of this section) than just at the definition-dependent characteristic points of them. The Bielefeld-Brookhaven-Columbia-Riken Collaboration [1] (independently of the observables) obtained T_c=192(4)(7) for physical quark masses in the continuum limit. The published results of the hotQCD Collaboration indicate a narrow transition within the 185–195 MeV temperature range (for which they expected about 5 MeV shift to smaller T values in the continuum limit and another 5 MeV because they used non-physical quark masses). Recent, preliminary results of the hotQCD Collaboration move closer and closer to our curves, and the original ≈40 MeV discrepancy in chiral variables is reduced to about 10 MeV (though the continuum extrapolated hotQCD result is missing). For a detailed comparison of our and their results see the next section.

[15]). The uncertainties are given in parentheses. The first one refers to $T > 0$, the second one to $T = 0$ statistical plus systematic errors.

5. Hadron Resonance Gas model

The Hadron Resonance Gas model has been widely used to study the low temperature phase of QCD in comparison with lattice data [20, 21, 22]. In Ref. [13] an important ingredient was included in this model, namely the pion mass- and lattice spacing-dependence of the hadron masses. In the present paper we combine these ingredients with Chiral Perturbation Theory (χPT) [23]. This opens the possibility to study chiral quantities, too.

5.1 The partition function of the HRG model

The low temperature phase of QCD is dominated by pions. Goldstone's theorem implies weak interactions between pions at low energies, which allows to study them within χPT. As the temperature T increases, heavier states become more relevant and need to be taken into account. The Hadron Resonance Gas model has its roots in the theorem by Dashen, Ma and Bernstein [24], which allows to calculate the microcanonical partition function of an interacting system, in the thermodynamic limit $V \to \infty$, to a good approximation, assuming that it is a gas of non-interacting free hadrons and resonances [25]. The pressure of the Hadron Resonance Gas model can be written as the sum of independent contributions

coming from non-interacting resonances

$$\frac{p^{HRG}}{T^4} = \frac{1}{VT^3} \sum_{i \in \, mesons} \ln Z^M(T, V, \mu_{X^a}, m_i) + \frac{1}{VT^3} \sum_{i \in \, baryons} \ln Z^B(T, V, \mu_{X^a}, m_i) \ , \quad (5.1)$$

where

$$\ln Z^M(T, V, \mu_{X^a}, m_i) = -\frac{V d_i}{2\pi^2} \int_0^\infty dk k^2 \ln(1 - z_i e^{-\varepsilon_i/T}),$$

$$\ln Z^B(T, V, \mu_{X^a}, m_i) = \frac{V d_i}{2\pi^2} \int_0^\infty dk \, k^2 \ln(1 + z_i e^{-\varepsilon_i/T}), \quad (5.2)$$

with energies $\varepsilon_i = \sqrt{k^2 + m_i^2}$, degeneracy factors d_i and fugacities

$$z_i = \exp\left((\sum_a X_i^a \mu_{X^a})/T \right) \ . \quad (5.3)$$

In the above equation, X^a are all possible conserved charges, including the baryon number B, electric charge Q and strangeness S. The sums in Eq. (5.1) include all known baryons and mesons up to 2.5 GeV, as listed in the latest edition of the Particle Data Book [26].

We will compare the results obtained with the physical hadron masses to those obtained with the distorted hadron spectrum which takes into account lattice discretization effects. As shown in Section 3.2, each pseudoscalar meson in the staggered formulation is split into 16 mesons with different masses. The contribution of each meson to the pressure is given by:

$$\frac{p^{\pi, K}}{T^4} = \frac{1}{16} \frac{1}{VT^3} \sum_{i=0}^{7} n_i \ln Z^M(T, V, \mu_{X^a}, m_i) \quad (5.4)$$

where m_i are the taste-split pseudoscalar meson masses (for the pion they are shown in Fig. 2) and n_i are the degeneracies listed in Table 1. Similarly to Ref. [13], we will also take into account the pion mass- and lattice spacing- dependence of all other hadrons and resonances.

In order to calculate the chiral condensate in the HRG model, we need to know the behavior of all baryon and meson masses as functions of m_l and m_s . For the quark mass-dependence of the ground state hadrons, we use the most recent fits from χPT available in the literature [27]. The same study is not available for all the resonances that we include. Therefore, similarly to Ref. [13], we work under the assumption that all resonance masses behave as their fundamental states as functions of m_q. In addition, in order to have a more precise estimate, we determine the contribution of pions to the chiral condensate obtained in three-loop chiral perturbation theory in [28]. All other hadrons and resonances are still treated in the ideal gas approximation. All details of this calculation are given in Appendix A. The HRG model + χPT results for light and strange quark number susceptibilities, and for the chiral condensate, are shown in Fig. 5.

It is instructive to look at these curves, before comparing them to the lattice results. In the low temperature phase, χ_2^u is dominated by pions, while χ_2^s by kaons; this is the
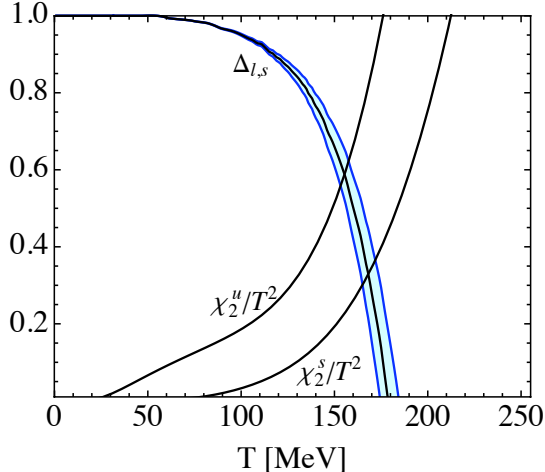
Figure 5: HRG + χPT results for the light and strange quark number susceptibilities and the subtracted chiral condensate $\Delta_{l,s}$. For this last quantity, the error band indicates the uncertainty on the quark mass-dependence of hadrons, see the Appendix. The results have been obtained with physical values for the hadron and resonance masses, thus no lattice artefact has been included.

reason why the light quark susceptibility rises much faster with increasing temperature, compared to the strange one. In the HRG model the susceptibilities keep increasing and $\Delta_{l,s}$ keeps decreasing to a negative value with increasing temperature. In QCD, all three quantities take values between 0 and 1. One can therefore take 0.5 as an illustration for the definition of T_c. From Fig. 5, it is evident that one obtains similar transition temperatures for $\Delta_{l,s}$ and χ_2^u, around 150 MeV, while χ_2^s reaches the 0.5 value at a larger temperature, around 170 MeV. From this figure it is also evident that it is not the mere value of T_c which is relevant in order to describe the phase transition, but rather the full temperature dependence of the curves, from which it is immediately clear that different observables may produce very different values for the transition temperature.

5.2 Comparison between HRG model and lattice results

In this paper we compare two sets of lattice data:

- The first set is based on the Wuppertal-Budapest results.

- The second set is obtained by the Bielefeld-Brookhaven-Columbia-Riken Collaboration, which later merged with a part of the the MILC collaboration and formed the hotQCD collaboration.

Furthermore, we use two types of theoretical description (based on hadron resonance gas model and chiral perturbation theory, for short: HRG+χPT):

- One of the theoretical descriptions is based on the physical spectrum from the Particle Data Book (we call this description "physical").

- The other theoretical approach is based on a non-physical spectrum (this spectrum is obtained by $T = 0$ simulations of the action one studies; the reason for this distortion will be explained later); we call this description "distorted".

As it is known, the Wuppertal-Budapest and the hotQCD results disagree. All characteristic temperatures are higher for the hotQCD Collaboration. Note, that this discrepancy is not related to the difficulty of determining e.g. inflection points of slowly varying functions (typical for a broad cross-over). The discrepancy appears for all variables for a large temperature interval. As we claimed earlier [8] we observed "approximately 20–35 MeV difference in the transition regime between our results and those of the hotQCD Collaboration".

As we will see, the Wuppertal-Budapest results are in complete agreement with the "physical" hadron resonance gas model and with the "physical" chiral perturbation theory, whereas the hotQCD results cannot be described this way. The hotQCD results can only be described by the "distorted" HRG+χPT.
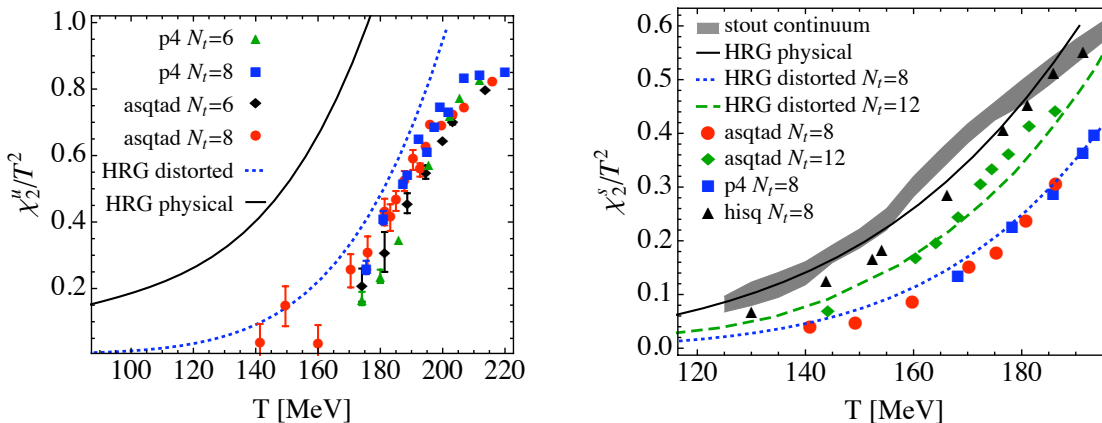

Figure 6: Left: light quark susceptibility as a function of the temperature. Right: strange quark susceptibility as a function of the temperature. In both panels, the points with different symbols correspond to results obtained with the asqtad and p4 actions [5, 11]. The solid line is the HRG model result with physical masses. The dashed and dotted lines are the HRG model results with distorted masses corresponding to $N_t = 12$ and $N_t = 8$, which take into account the discretization effects and heavier quark masses, which characterizes the results of the hotQCD Collaboration. Our continuum result for the strange susceptibility is shown by the band. Good agreement is found with the physical HRG+χPT results. (Due to the noisy contribution of the disconnected diagrams we have not determined the light quark susceptibility.)

In Fig. 6 we show the light and strange quark number susceptibilities, in the left and right panels, respectively. The lattice results are compared to the HRG model predictions for physical (solid line) and distorted (dashed line) spectrum (due to the noisy contribution of the disconnected diagrams we don't have results for the light quark susceptibility). The distorted spectrum takes into account the larger quark masses used by the hotQCD collaboration, as well as the larger lattice spacing and pseudoscalar meson splittings (see figure 2). For all hadrons and resonances, we use the pion mass- and lattice spacing-dependence given in Refs. [19, 29] and parametrized in Ref. [13]. As we can see, once

we take these effects into account (which corresponds to a distorted spectrum), the HRG curves on both figures are sensibly different from the physical ones and agree with the corresponding lattice data of hotQCD. Our continuum results on the strange susceptibility are compared to the other results, too. We observe a good agreement between our results and the "physical" HRG ones[4]. Notice that the agreement between lattice and HRG model results is good below the transition temperature, while for larger temperatures a deviation is obviously expected. This is observed both in our results and the hotQCD ones, but the temperatures at which deviations occur are obviously different.
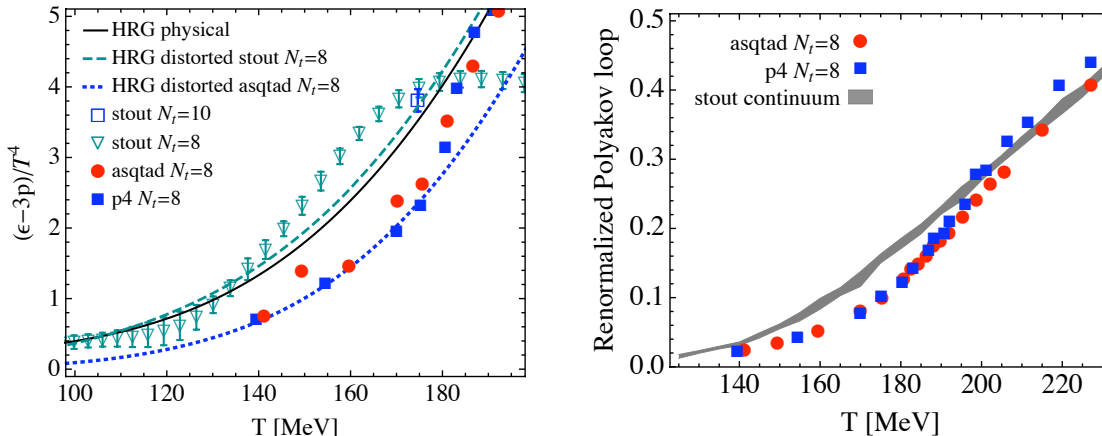

Figure 7: Left: $(\epsilon - 3p)/T^4$ as a function of the temperature. Open symbols are our results. Full symbols are the results for the asqtad and p4 actions at $N_t = 8$ [5]. Solid line: HRG model with physical masses. Dashed lines: HRG model with distorted spectrums. As it can be seen, the prediction of the HRG model with a spectrum distortion corresponding to the stout action at $N_t = 8$ is already quite close to the physical one. The error on the recent preliminary HISQ result [11] is larger than the difference between the stout and asqtad data, that is why we do not show them here. Right: renormalized Polyakov loop. We compare our results with those of the hotQCD Collaboration (asqtad and p4 data for $N_t = 8$ [5]).

In the left panel of Fig. 7 we show the trace anomaly divided by T^4 as a function of the temperature. Our $N_t = 8$ results are taken from Ref. [15]. Notice that, for this observable, we have a check-point at $N_t = 10$ too: the results are on top of each other. Also shown are the results of the hotQCD collaboration at $N_t = 8$ [5] and the HRG model predictions for physical and distorted resonance spectrums. On the one hand, our results are in good agreement with the "physical" HRG model ones. It is important to note, that using our mass splittings and inserting this distorted spectrum into the HRG model gives a temperature dependence which lies essentially on the physical HRG curve (at least within our accuracy). On the other hand, a distorted spectrum based on the asqtad and p4 frameworks results in a shift of about 20 MeV to the right. The asqtad and p4 lattice results can be successfully described by this distorted HRG prediction, too.

In the right panel of Fig. 7 we show the renormalized Polyakov loop (the renormalization procedure was discussed in the previous Section). The comparison with the data of

---

[4]For completeness we included in our comparisons preliminary [11] results of the hotQCD collaboration obtained by the HISQ and asqtad actions on N_t=8 and 12, respectively. We will discuss their impact later.

[5] shows a good agreement at high temperatures, and deviations in the transition region.

In Fig. 8, we show results for the chiral condensate as a function of the temperature. The left panel shows $\langle\bar{\psi}\psi\rangle_R$ as defined in Eq. (4.3), while the right panel shows $\Delta_{l,s}$ (see Eq. (4.4)). In both panels, the solid black curve has been obtained in the HRG+χPT model, using the equations given in Appendix A. The error bands of the theoretical lines correspond to the uncertainty in the quark mass dependence of hadron masses [27]. Gray bands correspond to our continuum results. They agree with the "physical" HRG+χPT predictions. In the right panel, we also show the lattice results for the subtracted chiral condensate obtained with the asqtad and p4 actions [5, 11]. These results are compared to the dashed curves, which have been obtained in the HRG+χPT model with "distorted" masses corresponding to $N_t = 8$ and $N_t = 12$. Also in this case, for all hadrons and resonances we use the pion mass- and lattice spacing-dependence taken from Refs. [19, 29] and parametrized in Ref. [13].

From all quantities that we have calculated, a consistent picture arises: our stout results agree with the "physical" HRG+χPT predictions; whereas the observed shift in transition temperatures between the results of the stout and the asqtad and p4 actions can be easily explained within the Hadron Resonance Gas+χPT model with "distorted" masses. Once the discretization effects, the taste violation and the heavier quark masses used in [5, 11] are taken into account, all the HRG+χPT curves for the different physical observables are shifted to higher temperatures and fall on the corresponding lattice results.

As a final check, we have determined the chiral condensate with larger quark masses ($m_s/m_{u,d} = 3$, corresponding to a pseudo-Goldstone mass of about 414 MeV and to an average pion mass of 587 MeV, which matches the one of Ref. [5] at $a = 0.183$ fm, corresponding to the lower end of the transition region $T = 135$ MeV at $N_t = 8$). Notice that, due to the reduced taste splitting of the stout action, we need $m_s/m_{u,d} = 3$ in order to have an average pion mass compatible with the one of Ref. [5], where $m_s/m_{u,d} = 10$. The results of this run are shown in Fig. 9. This procedure allows us to reproduce the results of the hotQCD collaboration for this observable, though with an artificially large quark mass. This example illustrates that a large pion splitting (of the asqtad action) results in a physically distorted spectrum, which can be mimicked by a small splitting (of the stout action) at an artificially large quark mass.

There is a proceedings contribution written by two members of the hotQCD Collaboration, in which the HISQ action is applied [10] and preliminary results are presented. This action uses a highly improved smearing recipe (and similarly to our stout action it reduces the pion splitting much more than the asqtad or p4 actions). In contrast to previous findings of the hotQCD collaboration, the results based on this new smeared improved action are quite close to our results. Both the strange susceptibility and the chiral condensate curves shift to lower temperatures. The approximately 20 MeV discrepancy for the strange susceptibility between the Wuppertal-Budapest and the hotQCD results has essentially disappeared. The approximately 35 MeV discrepancy for the chiral condensate curves is reduced to about 10 MeV (see Fig. 10). One expects that the results with the HISQ action will approach the continuum results much faster than those with the previously applied asqtad or p4 actions of the hotQCD collaboration. Note, that the continuum
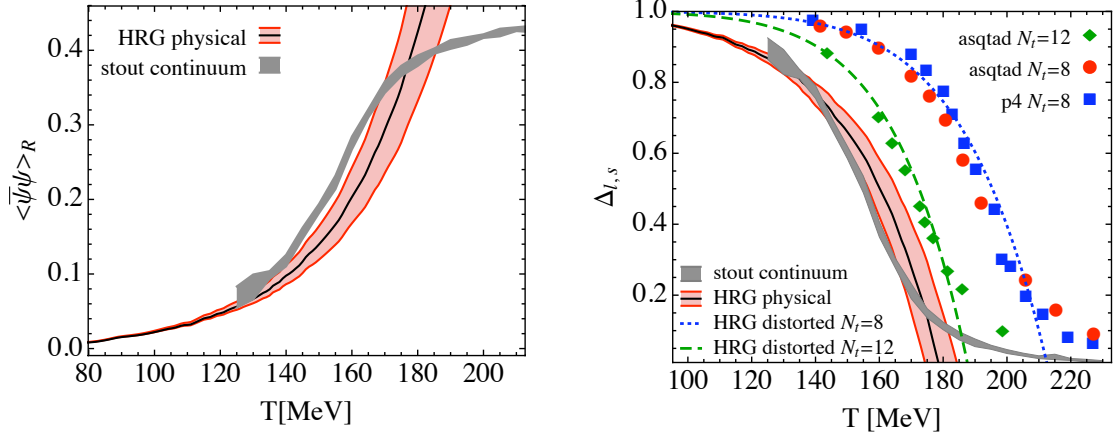
Figure 8: Left: Renormalized chiral condensate as defined in Eq. (4.3). Right: Subtracted chiral condensate $\Delta_{l,s}$ as defined in eq. (4.4), as a function of the temperature. Gray bands are the continuum results of our collaboration, obtained with the stout action. Full symbols are obtained with the asqtad and p4 actions [5, 11]. In both panels, the solid line is the HRG model result with physical masses. The error band corresponds to the uncertainty in the quark mass-dependence of hadron masses. The dashed lines are the HRG+χPT model result with distorted masses, which take into account the discretization effects and heavier quark masses used in [5, 11] for $N_t = 8$ and $N_t = 12$.
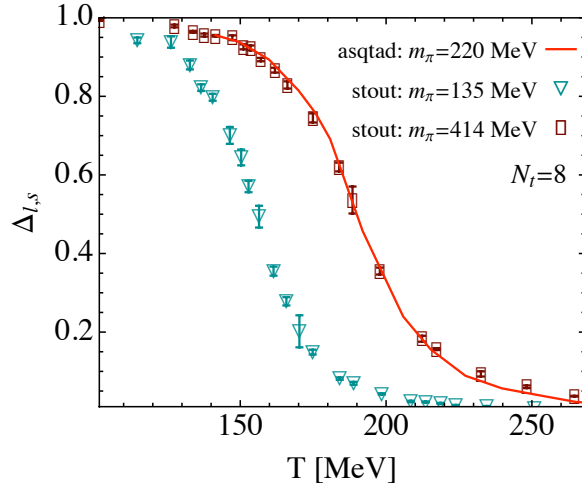

Figure 9: Subtracted chiral condensate $\Delta_{l,s}$ as a function of the temperature. The empty triangles are our results with physical quark masses as shown in Fig. 4. The empty rectangles are our results with an average pion mass of 587 MeV at $T \simeq 135$ MeV. The red curve is the result of the hotQCD collaboration [5]: these results are the same shown in Fig. 8: a line connects the data to lead the eye. For all sets of data we have $N_t = 8$. As it can be seen, the asqtad data can be mimicked in the stout framework by using a larger quark mass.

limit within the HISQ framework is still missing. This last important step (which needs quite some computational resources and also care) will hopefully eliminate the remaining minor discrepancy, too. The same two members of the hotQCD Collaboration presented

preliminary results using the asqtad action on N_t=12 lattices [11], too. At this lattice spacing the pion splitting is smaller than on N_t=8 lattices, and the curves move closer to ours. Since this action and lattice spacing combination has still a larger splitting than the HISQ result, it is further away from our continuum results than the findings within the HISQ framework. Following these two authors (Figure 5. of Ref. [11]) we zoom in into the transition region of $\Delta_{l,s}$ and on Figure 10 we show various findings. The stout results from a broad range of lattice spacings (N_t=8, 10, 12 and 16) are shown with open symbols. They all accumulated in the vicinity of our continuum estimate, indicated by the thin gray band. The hotQCD results were obtained by three different actions (p4, asqtad and HISQ) and with two different pion masses (220 and 160 MeV). They cover a broad range. The smaller the pion mass and/or pion splitting in the hotQCD results, the closer it is to ours.

These results confirm the expectations [7, 8] that the source of the discrepancy was the lack of the proper continuum extrapolation [7] in the hotQCD result: a dominant discretization artefact within the asqtad and p4 actions is the large pion splitting [12], which resulted in the distorted spectrum.

As we emphasized in both our previous studies [7, 8], only continuum extrapolated results are physical. We demonstrated [7] that using f_K and r_0 scale settings gives the same continuum result. Furthermore, we showed that using other quantities (the masses of the Ω, K^* and Φ hadrons or the pion decay constant) the same continuum result is obtained [8]. In this sense (thus after continuum extrapolation) one scale setting can be susbstituted by another one, the result remains the same. The ideal situation would be to compare our (continuum) results and the results obtained by continuum extrapolation based on HISQ (asqtad, p4 or any other) action. Without continuum extrapolation, cutoff effects appear, which can manifest themselves by providing different scales from different observables. As it is now, for the chiral condensate there is about 10 MeV difference between the continuum result of the Wuppertal-Budapest collaboration and the non-continuum N_t=8 results obtained by the HISQ action (Note, that this is much smaller than previous findings of the hotQCD Collaboration indicated). As we mentioned, carrying out the continuum extrapolation with the HISQ action will probably remove even this small difference.

6. Conclusions

We have presented our latest results for the QCD transition temperature. The quantities that we have studied are the strange quark number susceptibility, the Polyakov loop, the chiral condensate and the trace anomaly. We have given the complete temperature dependence of these quantities, which provide more information that the characteristic temperature values alone. Our previous results for the strange quark susceptibility, the Polyakov loop and the chiral condensate have been pushed to an even finer lattice ($N_t = 16$). The new data corresponding to $N_t = 16$ confirm our previous results. The trace anomaly [15] was obtained for $N_t = 8$ and a check-point at $N_t = 10$. The transition temperature that we obtain from this last quantity is very close to the one obtained from the chiral condensate.

In order to find the origin of the discrepancy between the results of our collaboration and the hotQCD ones, we calculated these observables (except the Polyakov loop) in the
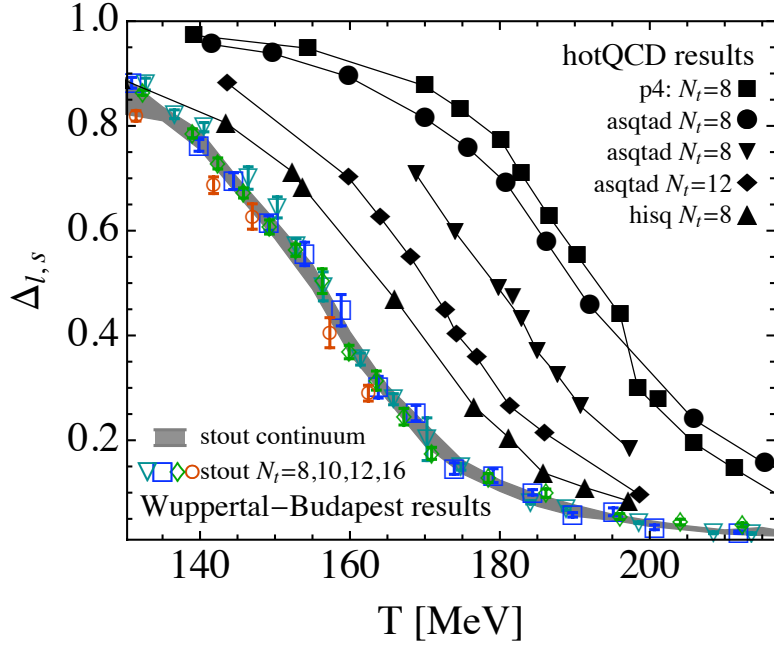
Figure 10: The subtracted chiral condensate $\Delta_{l,s}$ as a function of the temperature. We show a comparison between stout, asqtad, p4 and HISQ [5, 11] results. Our results are shown by colored open symbols, whereas the hotQCD results are shown by full black symbols. The gray band is our continuum result, the thin lines for the hotQCD data are intended to lead the eye. Our stout results were all obtained by the physical pion mass of 135 MeV. The full dots and squares correspond to $m_\pi = 220$ MeV, the full triangles and diamonds correspond to $m_\pi = 160$ MeV of the hotQCD collaboration.

Hadron Resonance Gas model. Besides using the physical hadron masses, we also performed the calculation with modified masses which take into account the heavier pions and larger lattice spacings used in [5]. We find an agreement between our data and the HRG ones with "physical" masses, while the hotQCD collaboration results are in agreement with the HRG model only if the spectrum is "distorted" as it was directly measured on the lattice [19, 29]. This analysis therefore provides an easy and convincing explanation of the observed shift in transition temperatures between the two collaborations and emphasizes the role of the proper continuum limit.

We used 2+1 flavor QCD within the staggered framework, which needs taking the root of the fermion determinant. There is a lively discussion in the literature whether this is a correct procedure. Though we have not seen any problem with this fermion formalism (our results and the predictions of the hadron resonance gas model agree very nicely up to the transition region) it is still very important to repeat the calculations with actions, which are free of the rooting problem (e.g. Wilson fermions).

Acknowledgements

Appendix

A. Renormalized chiral condensate

In order to calculate the subtracted chiral condensate $\Delta_{l,s}$ as defined in Eq. (4.4), we need to calculate $\langle\bar{\psi}\psi\rangle_{u,T}$ and $\langle\bar{\psi}\psi\rangle_{s,T}$. The light quark chiral condensate is given by:

$$\langle\bar{\psi}\psi\rangle_{u,T} = \langle\bar{\psi}\psi\rangle_{u,0} + \langle\bar{\psi}\psi\rangle_{\pi} + \frac{T}{V}\left[\sum_{i\in mesons}\frac{\partial\ln Z^M\left(T,V,\mu_{X^a},m_i\right)}{\partial m_i}\frac{\partial m_i}{\partial m_\pi^2}\frac{\partial m_\pi^2}{\partial m_u}\right.$$
$$\left.+\sum_{i\in baryons}\frac{\partial\ln Z^B\left(T,V,\mu_{X^a},m_i\right)}{\partial m_i}\frac{\partial m_i}{\partial m_\pi^2}\frac{\partial m_\pi^2}{\partial m_u}\right]. \tag{A-1}$$

In the above formula, $\langle\bar{\psi}\psi\rangle_{u,0}$ is the chiral condensate at vanishing temperature, $\langle\bar{\psi}\psi\rangle_{\pi}$ is the temperature-dependent pion contribution, that we take from the χPT investigation of Ref. [28]. The sum over mesons in the square brackets obviously does not include pions. The derivatives of the hadron masses with respect to m_π^2 can be written as:

$$\frac{\partial m_i}{\partial m_\pi^2} = \frac{\sigma_i}{(m_\pi^2)_{phys}} \tag{A-2}$$

where the σ_i are the sigma terms evaluated at the physical pion mass. We use for our analysis the results recently obtained in [27] for the fundamental states. They agree with the results obtained by our collaboration in [30]. We assume here that the resonances have the same sigma terms as their fundamental states. Using the notations of Ref. [28] we have:

$$\langle\bar{\psi}\psi\rangle_{u,0} = \frac{m_\pi^2}{2m_u}\frac{F^2}{c} \quad\Rightarrow\quad m_\pi^2 = 2\frac{\langle\bar{\psi}\psi\rangle_{u,0}cm_u}{F^2} \quad\Rightarrow\quad \frac{\partial m_\pi^2}{\partial m_u} = 2\frac{\langle\bar{\psi}\psi\rangle_{u,0}c}{F^2} \tag{A-3}$$

In the above formulas, c is a temperature-independent constant which is equal to 1 in the massless theory. The corrections of order m_q have been calculated and give

$$c = 0.90 \pm 0.05; \tag{A-4}$$

F is the pion decay constant in the chiral limit:

$$F = 88.3 \pm 1.1\text{MeV}. \tag{A-5}$$

Therefore, replacing the above relations in Eq. (A-1), we obtain:

$$\langle\bar\psi\psi\rangle_{u,T} = \langle\bar\psi\psi\rangle_{u,0}\left\{1 + \frac{\langle\bar\psi\psi\rangle_\pi}{\langle\bar\psi\psi\rangle_{u,0}} + 2\frac{c}{F^2}\frac{T}{V}\left[\sum_{i\in mesons}\frac{\partial\ln Z^M\left(T,V,\mu_{X^a},m_i\right)}{\partial m_i}\frac{\sigma_i}{(m_\pi^2)_{phys}}\right.\right.$$

$$\left.\left. + \sum_{i\in baryons}\frac{\partial\ln Z^B\left(T,V,\mu_{X^a},m_i\right)}{\partial m_i}\frac{\sigma_i}{(m_\pi^2)_{phys}}\right]\right\} \tag{A-6}$$

We now need to calculate the strange quark condensate, $\langle\bar\psi\psi\rangle_{s,T}$. We proceed in a similar way as for the light quark condensate:

$$\langle\bar\psi\psi\rangle_{s,T} = \langle\bar\psi\psi\rangle_{s,0} + \langle\bar\psi\psi\rangle_K + \frac{T}{V}\left[\sum_{i\in mesons}\frac{\partial\ln Z^M\left(T,V,\mu_{X^a},m_i\right)}{\partial m_i}\frac{\partial m_i}{\partial m_s}\right.$$

$$\left. + \sum_{i\in baryons}\frac{\partial\ln Z^B\left(T,V,\mu_{X^a},m_i\right)}{\partial m_i}\frac{\partial m_i}{\partial m_s}\right]. \tag{A-7}$$

$\langle\bar\psi\psi\rangle_{s,0}$ is the zero-temperature value of the strange condensate, which is related to $\langle\bar\psi\psi\rangle_{u,0}$ by QCD sum rules [31]:

$$\langle\bar\psi\psi\rangle_{s,0} = 0.8\langle\bar\psi\psi\rangle_{u,0} \tag{A-8}$$

$\langle\bar\psi\psi\rangle_K$ is the kaon contribution to the strange condensate:

$$\langle\bar\psi\psi\rangle_K = \frac{\partial\ln Z^M\left(T,V,\mu_{X^a},m_K\right)}{\partial m_K}\frac{\langle\bar\psi\psi\rangle_{u,0}c}{2m_KF^2}. \tag{A-9}$$

The strange mass dependence of hadrons and resonances can be written as:

$$\frac{\partial m_i}{\partial m_s} = \frac{\sigma_{i,s}}{m_s} = \sigma_{i,s}\frac{\langle\bar\psi\psi\rangle_{u,0}c}{m_K^2F^2}\frac{m_u+m_s}{m_s}; \tag{A-10}$$

the sigma terms $\sigma_{i,s}$ involving strange quarks are taken from Ref. [27]. The sum over mesons in the square brackets of Eq. (A-7) does not include kaons.

The ratio $(m_u+m_s)/m_s$ is equal to $29.15/28.15$ for our collaboration, and to $11/10$ or $21/20$ for the hotQCD collaboration. We therefore have:

$$\langle\bar\psi\psi\rangle_{s,T} = \langle\bar\psi\psi\rangle_{u,0}\left\{0.8 + \frac{\partial\ln Z^M\left(T,V,\mu_{X^a},m_i\right)}{\partial m_K}\frac{c}{2m_KF^2}\right.$$

$$+ \frac{T}{V}\frac{c}{m_K^2F^2}\frac{m_u+m_s}{m_s}\left[\sum_{i\in mesons}\frac{\partial\ln Z^M\left(T,V,\mu_{X^a},m_i\right)}{\partial m_i}\sigma_{i,s}\right.$$

$$\left.\left. + \sum_{i\in baryons}\frac{\partial\ln Z^B\left(T,V,\mu_{X^a},m_i\right)}{\partial m_i}\sigma_{i,s}\right]\right\} \tag{A-11}$$

B. Continuum results

In this paper we presented lattice data with $N_t = 8, 10, 12$ and 16. Our continuum extrapolation is based on these resolutions assuming a $\sim 1/N_t^2$ behaviour. We used a fitted spline interpolation on the data. We summarize the results in Table 3.

In order to determine the transition temperatures we followed Ref. [30] and applied a combined fitting method weighting among various scenarios. The result is a robust estimate. Note that the inflection points obtained using this method do not necesserily agree with the inflection point of the mean values of Table 3. Clearly, in an almost straight band (T dependent results with error bars) one can draw various curves with different inflection points. That is the reason, why we emphasize more the complete temperature dependence than the individual T_c values.

T [MeV]	χ_2^s/T^2	L_{Polyakov}	$\langle\bar{\psi}\psi\rangle_R$	$\Delta_{l,s}$
125	0.08(1)	0.015(3)	0.07(1)	0.89(3)
130	0.10(2)	0.022(2)	0.08(2)	0.85(4)
135	0.12(2)	0.028(2)	0.099(5)	0.81(1)
140	0.14(2)	0.033(3)	0.118(8)	0.76(2)
145	0.18(2)	0.045(4)	0.155(8)	0.67(2)
150	0.20(2)	0.059(4)	0.188(6)	0.59(1)
155	0.24(2)	0.073(6)	0.223(9)	0.49(3)
160	0.30(2)	0.091(8)	0.276(9)	0.37(2)
165	0.35(2)	0.109(6)	0.315(6)	0.28(1)
170	0.40(2)	0.13(1)	0.350(8)	0.20(2)
175	0.44(2)	0.157(7)	0.372(7)	0.14(1)
180	0.48(2)	0.178(7)	0.386(7)	0.11(1)
185	0.51(2)	0.199(7)	0.399(4)	0.08(1)
190	0.55(2)	0.226(6)	0.408(6)	0.063(9)
195	0.59(2)	0.25(1)	0.413(5)	0.051(5)
200	0.63(2)	0.276(6)	0.419(3)	0.039(5)
205	0.65(2)	0.300(6)	0.424(5)	0.031(4)
210	0.68(2)	0.326(7)	0.428(3)	0.024(4)
215	0.70(2)	0.350(7)	0.429(4)	0.023(4)
220	0.73(2)	0.38(1)	0.433(3)	0.018(3)

Table 3: The continuum behaviour of our observables in the transition region (please note that there is an uncertainty of about 2% in the temperature values corresponding to the systematics of setting the scale).

References

[1] M. Cheng *et al.*, Phys. Rev. D **74**, 054507 (2006) [arXiv:hep-lat/0608013].

[2] C. E. Detar and R. Gupta [HotQCD Collaboration], PoS **LAT2007**, 179 (2007) [arXiv:0710.1655 [hep-lat]].

[3] F. Karsch, PoS **LAT2007**, 015 (2007) [arXiv:0711.0661 [hep-lat]].

[4] F. Karsch [RBC Collaboration and HotQCD Collaboration], J. Phys. G **35**, 104096 (2008) [arXiv:0804.4148 [hep-lat]].

[5] A. Bazavov *et al.*, Phys. Rev. D **80**, 014504 (2009) [arXiv:0903.4379 [hep-lat]].

[6] M. Cheng *et al.*, Phys. Rev. D **81**, 054504 (2010) [arXiv:0911.2215 [hep-lat]].

[7] Y. Aoki, Z. Fodor, S. D. Katz and K. K. Szabo, Phys. Lett. B **643**, 46 (2006) [arXiv:hep-lat/0609068].

[8] Y. Aoki, S. Borsanyi, S. Durr, Z. Fodor, S. D. Katz, S. Krieg and K. K. Szabo, JHEP **0906**, 088 (2009) [arXiv:0903.4155 [hep-lat]].

[9] Y. Aoki, G. Endrodi, Z. Fodor, S. D. Katz and K. K. Szabo, Nature **443**, 675 (2006) [arXiv:hep-lat/0611014].

[10] A. Bazavov and P. Petreczky, PoS **LAT2009**, 163 (2009) [arXiv:0912.5421 [hep-lat]].

[11] A. Bazavov and P. Petreczky, arXiv:1005.1131 [hep-lat].

[12] Z. Fodor, PoS **LAT2007** (2007) 011 [arXiv:0711.0336 [hep-lat]].

[13] P. Huovinen and P. Petreczky, Nucl. Phys. A **837** (2010) 26 [arXiv:0912.2541 [hep-ph]]. P. Huovinen and P. Petreczky, arXiv:1005.0324 [hep-ph].

[14] B. Spang, http://www.cheresources.com/iapwsif97.shtml

[15] S. Borsányi, G. Endrődi, Z. Fodor, A. Jakovác, S. Krieg, C. Ratti, K. K. Szabó "The QCD equation of state with dynamical quarks", WUB/10-12

[16] Y. Aoki, Z. Fodor, S. D. Katz and K. K. Szabo, JHEP **0601**, 089 (2006) [arXiv:hep-lat/0510084].

[17] C. Morningstar and M. J. Peardon, Phys. Rev. D **69**, 054501 (2004) [arXiv:hep-lat/0311018].

[18] M. F. L. Golterman, Nucl. Phys. B **273**, 663 (1986); Nucl. Phys. B **278**, 417 (1986).

[19] A. Bazavov *et al.*, arXiv:0903.3598 [hep-lat].

[20] F. Karsch, K. Redlich and A. Tawfik, Eur. Phys. J. C **29**, 549 (2003) [arXiv:hep-ph/0303108].

[21] F. Karsch, K. Redlich and A. Tawfik, Phys. Lett. B **571**, 67 (2003) [arXiv:hep-ph/0306208].

[22] A. Tawfik, Phys. Rev. D **71**, 054502 (2005) [arXiv:hep-ph/0412336].

[23] J. Gasser and H. Leutwyler, Annals Phys. **158** (1984) 142.

[24] R. Dashen, S. K. Ma and H. J. Bernstein, Phys. Rev. **187**, 345 (1969).

[25] R. Venugopalan and M. Prakash, Nucl. Phys. A **546**, 718 (1992).

[26] C. Amsler et al. (Particle Data Group), Physics Letters B **667**, 1 (2008) and 2009 partial update for the 2010 edition.

[27] J. Martin-Camalich, L. S. Geng and M. J. V. Vacas, arXiv:1003.1929 [hep-lat].

[28] P. Gerber and H. Leutwyler, Nucl. Phys. B **321**, 387 (1989).

[29] C. Aubin *et al.*, Phys. Rev. D**70**, 094505 (2004) [arXiv:hep-lat/0402030]; C. W. Bernard *et al.*, Phys. Rev. D**64**, 054506 (2001) [arXiv:hep-lat/0104002].

[30] S. Durr *et al.*, Science **322**, 1224 (2008) [arXiv:0906.3599 [hep-lat]].

[31] M. Jamin, Phys. Lett. B **538**, 71 (2002) [arXiv:hep-ph/0201174].

[32] C. Bernard, M. Golterman, Y. Shamir and S. R. Sharpe, Phys. Rev. D **77**, 114504 (2008) [arXiv:0711.0696 [hep-lat]].